

Stereo Matching Algorithm for 3D Surface Reconstruction Based on Triangulation Principle

*Rostam Affendi Hamzah, **Haidi Ibrahim, ***Anwar Hasni Abu Hassan

School of Electrical & Electronic Engineering
Engineering Campus, Universiti Sains Malaysia,
14300 Nibong Tebal
Penang, Malaysia

Email: *rostamaffendi@utem.edu.my, **haidi_ibrahim@ieee.org, ***eeanwar@usm.my

Abstract—This article presents a new stereo matching algorithm based on local method. The absolute difference (AD) algorithm works fast and precise at low texture area, however this algorithm is sensitive to radiometric distortions (i.e., contrast or brightness) and low texture areas. To overcome these problems, the proposed algorithm utilizes a combination of AD, gradient difference (GM) and census transform (CT). The GM algorithm is robust against the radiometric errors and CT algorithm works well on the low texture regions. The proposed algorithm performs much better based on the experimental results of the Middlebury dataset. The disparity map from the result consists of depth information which requires for the three-dimensional (3D) surface reconstruction.

I. INTRODUCTION

Stereo matching is a work of establishing the correspondence between a pair of images. The output from this process is known as disparity map. The depth from the disparity map is important for numerous fields such as virtual reality and robotics. A precise disparity map is able to assist robots to maneuver in actual situation. Moreover, the realistic world, disparity maps bring on a significant function in three-dimensional (3D) reconstruction from the input images. Disparity map shows crucial 3D information for assigning the image pixels to precisely produce the depth of the dissimilar detected objects when looking at the contrastive perspectives [1]. Yet, depth estimation for disparity map is one of the most challenging and delicate problems. In the past years, many researches have been done to handle this difficulty and good improvements have been succeeded. The disparity map estimation comprises of finding the correspondence for each pixel pair from two images. According to the taxonomy proposed by Scharstein and Szeliski [2], there are four steps to develop a stereo matching algorithm:

- Step 1: Matching cost computation (i.e., Matching process at each pixel of left and right images)
- Step 2: Cost aggregation (i.e., Aggregate initial costs over support region)
- Step 3: Disparity optimization (i.e., Select the disparity level that optimized the function)
- Step 4: Disparity refinement (i.e., Post-processing to refine the disparity map)

The disparity map development can be classified as global or local optimization method. This classification is based on the technique on how the disparity is calculated [3]. Local approaches use the disparity based on the correspondence between the pixel intensities (i.e., gray-scale, RGB colors, texture patterns) inside a given local support window. These approaches are also referred as window-based or region-based methods. There are several approaches related to the window-based such as fixed window [4], multiple window [5] and adaptive window [6]. The methods use only local data. Hence, they have a modest computational requirement and low runtime. The disparity map is generated by choosing the smallest matching cost from disparity candidates. This selective technique is named as winner takes all (WTA) [7]. The execution of the local method produces fast runtime. However, the quality is low, particularly in the region of depth discontinuity.

On the other hand, global approaches determine the disparity based on the minimizing a predefined global energy function [8]. The measurement is taken from the global data and a smoothness constraint from the neighbouring pixels [1]. The smooth function is utilized in the same region while at the same time refines the object boundaries. There were several techniques in global energy minimization which uses a graph-based approach from Markov Random Field (MRF). These techniques include graph cut (GC) method [9] and belief propagation method [10]. The GC method applies the MRF approach with a max-flow algorithm and minimum cut to the energy flow composition. In contrast, the belief propagation method uses the MRF graph by repetitively passing messages from the current node to neighboring nodes. Global methods can obtain great accuracy. Unfortunately they have high computational requirement.

This paper proposes a combination of matching cost functions to calculate more accurately the disparity map. The proposed local-based algorithm uses a combination of three different similarity measurements. It consists of absolute difference (AD), gradient difference (GM) and census transform (CT). The aggregation step implemented using a guided filter as proposed by He et al. [11]. The post-processing stage uses the left-right consistency checking process to detect the

invalid pixels and a bilateral filter to smooth the final disparity maps. From the proposed algorithm, the accuracy level is increased. This article is organized as follows. Section II discusses previous works in more details. Section III explains the proposed stereo matching algorithm. Section IV demonstrates the experimental arrangements and results. The conclusion is given in Section V.

II. RELATED WORKS ON LOCAL STEREO MATCHING ALGORITHM

Recently, numerous local methods have been developed to obtain a disparity map [12]. There are some regularly used similarity cost matching function through the window-based techniques. They are the sum of absolute differences (SAD) [13], sum of squared differences (SSD) and normalized cross correlation (NCC) [14]. It is observed from all of these works that the main problem of window based technique is they normally assume that the pixels inside the support region are having equal disparities. Actually, it is certainly not effectual for pixels near edges or depth discontinuities. Hence, incorrect deciding of the shape and size of the matched window leads to wrong disparity value approximations. In the work by Hu et al. [15], the virtual support window was introduced which developed more complex solution to resize the support windows. Another complex solution was proposed by Inecke and Eggert [16] that implemented a modification of normalized cross correlation (NCC) algorithm at matching stage. Generally, local approaches show low quality at those areas because of inappropriate assortment of the selected window radius.

In previous development, the stage of cost aggregation (i.e., Step 2), the adaptive support weight (ASW) techniques [17] acquired consideration because of good quality of disparity map estimations. This approach delivers intensity similarity on weighting between the support window. Therefore, for every pixel, ASW marks the neighbouring pixels which have higher support during the aggregation process. ASW offers a constant weight sharing for smooth areas, thus maximizing characteristic against noise and able to preserve the edge features. However, support weight methods require individual computation for every pixel in the neighborhood that will increase computational cost and huge amount of memory. Moreover, in the work of Kowalczyk et al. [6], two-stage adaptive support weights (ASW) algorithms have been used, with a combination of iterative refinement technique and ASW based cost aggregation stage. Their work produces high accuracy. However, the complexity of their work was also high as it used ASW and iterative approaches in the same algorithm. ASW approach requires high computational complexity to adaptively determine the shape or texture.

Two established local disparity refinement techniques are median filtering and Gaussian convolution. In the work by Michael et al. [18], the disparity map refinement stage which used median filter was developed for real time stereo vision algorithm. Furthermore, modifications on median filter done by Ma et al. [19] which used a constant time weighted technique.

Their results are shown high accuracy in removing noise and error with respect to the edge of disparity map produced. Another approach is the Gaussian convolution which aggregates a disparity estimation with those of its neighbours, accordant to weights formed by a Gaussian distribution. This method decreases the noise on the disparity map. Unfortunately the Gaussian filter also decreases the amount of fine detail existing in the final disparity map.

III. THE PROPOSED STEREO MATCHING ALGORITHM

The development of the proposed algorithm takes the steps as illustrated in Fig. 1. The matching cost computation uses the AD, GM and CT as a pixel based correspondence measurements. The cost aggregation is implemented using a guided filter. Then, the disparity optimization with WTA strategy is absorbed by using the minimum aggregated corresponding value for every valid pixel. The left-right cross consistency checking is applied to discover the invalid regions due to occlusion or matching error at untextured area. To get rid of invalid pixels, the filling process is take place. The minimum value of a valid pixel is chosen to replace the invalid pixels. The final stage consists of implementing the bilateral filter to remove the remaining noise which usually occur in previous filling process.

A. Matching Cost Computation

In this sub-section, the proposed pixel-based matching stage is using a combination of three pixel-based similarity measurements. The $AD(p, d)$, which relies only on the intensity difference of two corresponding pixels in RGB channels on the left image I_l and right image I_r is given by Equation (1):

$$AD(p, d) = \sum_{i \in \{R, G, B\}} |I_l^i(p) - I_r^i(p - d)| \quad (1)$$

where the pixel of interest coordinates (x, y) represented by p , i denotes the RGB channels number and d is disparity value. The condition while applying the final absolute differences $AD'(p, d)$ is given by Equation (2):

$$AD'(p, d) = \begin{cases} \tau_{AD}, & \text{if } AD_{new}(p, d) > \tau_{AD}, \\ AD_{new}(p, d), & \text{otherwise.} \end{cases} \quad (2)$$

where τ_{AD} denotes the truncated value as implemented by [20] to increase the robustness against the outliers. Meanwhile, the gradient components for each image in horizontal direction G_x and vertical direction G_y are given by Equation (3) and Equation (4):

$$G_x = [1 \quad 0 \quad -1] * I \quad (3)$$

$$G_y = \begin{bmatrix} 1 \\ 0 \\ -1 \end{bmatrix} * I \quad (4)$$

where I is the image and $*$ is the convolution operation. Using both gradient components, the gradient magnitude m is given by Equation (5):

$$m = \sqrt{G_x^2 + G_y^2} \quad (5)$$

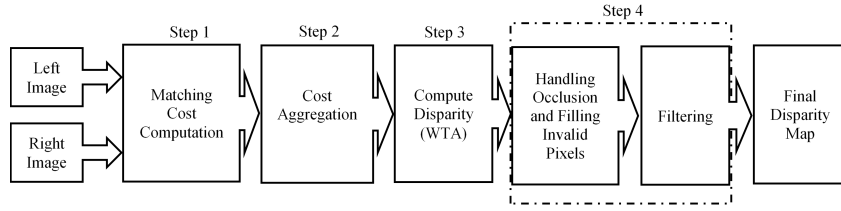


Fig. 1. A stereo matching system.

The modulus of gradient operator in Equation (5) is applied to the left gray image m_l and right gray image m_r respectively. In the x -direction of gradient displacement with a static position of y -direction, the gradient matching cost $GM(p, d)$ is given by Equation (6):

$$GM(p, d) = |m_l(p) - m_r(p - d)| \quad (6)$$

where the pixel of interest's coordinates is p and d denotes the disparity value. The final value of the gradient difference depends on the value which is not exceed the truncated value at τ_{GM} . This is shown by Equation (7):

$$GM'(p, d) = \begin{cases} \tau_{GM}, & \text{if } |GM_{new}(p, d)| > \tau_{GM}, \\ |GM_{new}(p, d)|, & \text{otherwise.} \end{cases} \quad (7)$$

The matching cost function $M'(p, d)$ at this stage is the combination of $AD'(p, d)$ and $GM'(p, d)$ which is given by Equation (8):

$$M'(p, d) = \alpha AD'(p, d) + (1 - \alpha) GM'(p, d) \quad (8)$$

where the α is added to control the gradient and color terms. The α controls the sensitivity to radiometric differences. In this work, the matching cost is added with the census transform volume. This makes the final matching cost volume robust against the illumination changes. The census transform uses local information which computes the Hamming distance of the bit string as given by Equation (9):

$$CN(p) = \otimes_{q \in w_{CN}} cen(p, q) \quad (9)$$

where \otimes operator refers to the bit-wise operation, p and q denote the pixel of interest and neighbouring pixels respectively. The w_{CN} is a support window and $cen(p, q)$ represents the binary function with the conditions as given by Equation (10):

$$cen(p, q) = \begin{cases} 1, & I(p) \geq I(q), \\ 0, & \text{otherwise.} \end{cases} \quad (10)$$

where $I(p)$ and $I(q)$ are the pixel of interest and neighbouring pixel values respectively. The Hamming distance is used to calculate the difference between two bit strings (i.e., left and right images) which is given by Equation (11):

$$CN'(p, d) = \text{Hamming}(CN_l(p) - CN_r(p - d)) \quad (11)$$

where CN_l and CN_r are the bit strings of left and right images respectively. The final matching cost function $M(p, d)$

is given by Equation (12) which uses normalised cost function as implemented by [21].

$$M(p, d) = 2 - \exp(-M'(p, d)) - \exp(-CN'(p, d)) \quad (12)$$

B. Cost Aggregation

This stage is the most critical and significant process which minimizing the matching uncertainties. It produces the overall performance of the disparity map for local methods. From cost matching step, the raw disparity values are very large and too sensitive to noise. In this work, the guided filter is selected because this filter is developed to reduce the noise and preserve the edges. The left image is selected in this paper as a reference and guidance to the process of filtering. The guided filter is given by Equation (13).

$$G_{p,q}(I) = \frac{1}{|w|^2} \sum_{q \in w_k} \left(1 + \frac{(I_p - \mu_k)(I_q - \mu_k)}{\sigma_k^2 + \epsilon} \right) \quad (13)$$

I is the guidance grayscale image. The (x, y) coordinates are replaced by p which represents the coordinates pixel of interest in support window. The σ and μ are the intensity value of variance and mean in a squared window of w_k with q indicates the neighbour pixels which centred at pixel k . The w represents number of pixels in square window of w_k . The ϵ value represents the control element for smoothness term. The aggregation cost at this step is given by Equation (14).

$$C(p, d) = \sum_q G_{p,q}(I) M(p, d) \quad (14)$$

C. Disparity Optimization

To obtain the accurate disparity map, this work computes final disparity by choosing the minimum aggregated corresponding value for every pixel utilized the WTA strategy. The utilization of WTA strategy at this stage in local algorithms. Through their findings, the disparity maps attained at this process still encounter unmatched pixels or invalid pixels in the occluded regions. Given Equation (15), the disparity related to the minimum aggregated cost d_p at each pixel is chosen. $C(x, y, d)$ means the cost aggregation acquired after the process of cost aggregation and D represents the set of all valid which allows discrete disparity values.

$$d_p = \text{argmin}_{d \in D} C(p, d) \quad (15)$$

D. Post-processing

This final stage of the proposed algorithm consists of occlusion handling, filling invalid pixels and filtering. The occlusion detection is discovered by left-right consistency check. This process is implemented from left to right disparity map image coincides with the disparity map calculated from the right to the left disparity map image. The result of this process is the invalid and rejected pixels due to occluded area or pixels at the plain regions. These invalid pixels are replaced with a valid minimum value of the nearest of disparity value. It should situated in the same scan line. Nevertheless, this filling and replacing process will create unwanted pattern artifacts on the disparity map. To remove that noise, the weighted of bilateral filter is utilized as given by Equation 16. This filter is an edge-preserving filter and is able to improve the disparity map quality.

$$WM_{p,q}^{BF} = exp\left(-\frac{|p-q|^2}{\sigma_s^2}\right)exp\left(-\frac{|I_p-I_q|^2}{\sigma_c^2}\right) \quad (16)$$

where p is a pixel needs to be denoised using the weight of the neighbouring pixel of q . The σ_s represents a spatial adjustment parameter and σ_c corresponds to the color similarity parameter. The $p-q$ refer to spatial Euclidean distance and $|I_p-I_q|$ is the Euclidean distance in color space.

E. 3D Surface Reconstruction

The 3D reconstruction is based on the triangulation principle as shown by Fig. 2 to estimate the depth Z given by Equation 17.

$$\frac{b}{Z} = \frac{(b+x_r)-x_l}{Z-f} \quad (17)$$

where $\{Z, b, x_l, x_r, f\}$ denote as $\{\text{depth, stereo camera baseline, left plane coordinate, right plane coordinate, focal length}\}$ respectively. The disparity d and depth Z are given by Equation (18) and Equation (19).

$$d = x_l - x_r \quad (18)$$

$$Z = \frac{bf}{d} \quad (19)$$

IV. EXPERIMENTAL RESULTS

The experiments are carried out on the platform of Window 10 on desktop PC with 3.2GHz processor and 8GB memory. To evaluate the accuracy, the experimental images are using a standard online benchmarking dataset from the Middlebury. This dataset consists of 15 training images. The accuracy is measured from the bad pixel percentage of non-occluded pixel (*nonocc*) and all pixels (*all*). The parameters used in this work were $\{\tau_{AD}, \tau_{GM}, \alpha, w_{CN}, w_k, \epsilon, \sigma_s, \sigma_c\}$ with the values of $\{0.02, 0.008, 0.18, 7 \times 7, 9 \times 9, 0.0001, 17, 0.3\}$. To test the effectiveness of the combined matching costs, the experiment on a single matching cost (i.e., TestAD) was also conducted with the same parameter settings in the framework. Fig. 3 shows the 15 training images, ground truth and the disparity map results after submitted to [22]. Based on the final results

of disparity maps, the scene objects situated at increasing depth are assigned step by step to disparity values from nearer to further based on the colours assignment.

Table I and II show the quantitative results of the Middlebury dataset. It shows that the proposed work is more accurate than the TestAD (i.e., with the weight average difference *nonocc*=13.15, *all*=19.11). The achievement of the proposed work has been analyzed with other local algorithms in [22]. Based on the results, the proposed algorithm is among the lowest of average errors which indicates the competitive achievement of the proposed work. Fig. 4 shows the results of 3D surface reconstruction based on depth information from the 2D disparity mapping. The disparity map used in the reconstruction was a grayscale image. It shows that the higher intensity value of pixels, the closer an object to the stereo vision camera. Based on the disparity maps input, the proposed algorithm displays more reliable surface reconstruction which more pixels are correctly mapped compared to TestAD algorithm. The TestAD algorithm produces high errors especially on the low texture regions on the wall behind the sitting chair.

V. CONCLUSION

In this paper, a local-based stereo matching algorithm is given. The experimental results demonstrated that the proposed method has improved the accuracy. The proposed algorithm is able to overcome the limitations of the AD algorithm. The guided filter is used at the aggregation stage due to its edge-preserving property. The optimization stage implemented using WTA strategy with a minimum value of disparities is selected. The left-right consistency checking and bilateral filter at the post-processing stage reduces existing noise that smoothed the final disparity map. The information from 2D disparity mapping can be used for 3D surface reconstruction based on the triangulation principle.

ACKNOWLEDGEMENT

This work was supported by Universiti Sains Malaysia and Universiti Teknikal Malaysia Melaka.

REFERENCES

- [1] Y.-C. Wang, C.-P. Tung, and P.-C. Chung, "Efficient disparity estimation using hierarchical bilateral disparity structure based graph cut algorithm with a foreground boundary refinement mechanism," *IEEE Transactions on Circuits and Systems for Video Technology*, vol. 23, no. 5, pp. 784–801, 2013.
- [2] D. Scharstein and R. Szeliski, "A taxonomy and evaluation of dense two-frame stereo correspondence algorithms," *International Journal of Computer Vision*, vol. 47, no. 1, pp. 7–42, 2002.
- [3] C. Shi, G. Wang, X. Yin, X. Pei, B. He, and X. Lin, "High-accuracy stereo matching based on adaptive ground control points," *IEEE Transactions on Image Processing*, vol. 24, no. 4, pp. 1412–1423, 2015.
- [4] Q. Yang, P. Ji, D. Li, S. Yao, and M. Zhang, "Fast stereo matching using adaptive guided filtering," *Image and Vision Computing*, vol. 32, no. 3, pp. 202–211, 2014.
- [5] H. Hirschmüller, P. R. Innocent, and J. Garibaldi, "Real-time correlation-based stereo vision with reduced border errors," *International Journal of Computer Vision*, vol. 47, no. 1-3, pp. 229–246, 2002.
- [6] J. Kowalczyk, E. T. Psota, and L. C. Perez, "Real-time stereo matching on cuda using an iterative refinement method for adaptive support-weight correspondences," *IEEE Transactions on Circuits and Systems for Video Technology*, vol. 23, no. 1, pp. 94–104, 2013.

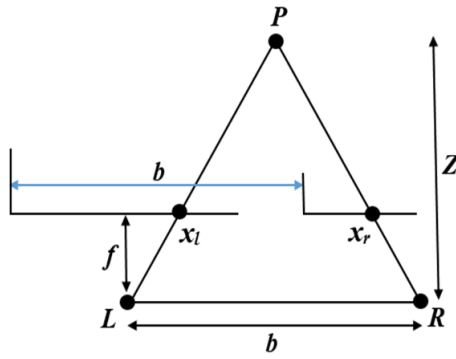


Fig. 2. Depth perception from two-dimensional (2D) of stereo geometry. The y-axis is fixed and the disparity is calculated based on the differences of x-axis.

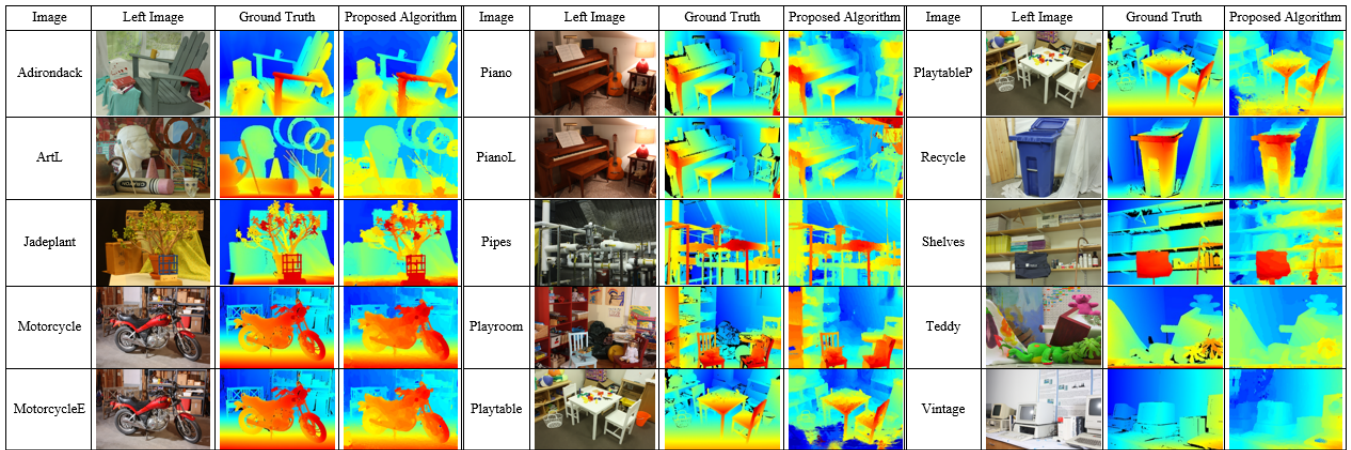


Fig. 3. The results of the Middlebury datasets.

TABLE I
THE COMPARISON RESULTS OF *nonocc* ERROR USING THE MIDDLEBURY DATASET.

Algorithms	Adiron	ArtL	Jadepl	Motor	MotorE	Piano	PianoL	Pipes	Playrm	Playt	PlayP	Recyc	Shelvs	Teddy	Vintge	Weight Ave
MC-CNN [23]	0.76	2.55	16.30	1.27	1.27	1.83	5.07	2.29	2.27	3.11	3.03	2.48	4.41	1.12	14.80	3.82
Proposed Algorithm	3.58	4.55	12.80	3.48	3.37	5.60	12.70	5.92	5.04	18.10	4.61	3.36	8.64	2.49	8.45	6.10
SNCC [16]	2.89	4.05	18.10	2.68	2.52	3.52	7.08	6.14	5.64	45.40	3.13	2.90	7.59	1.58	13.50	6.97
ELAS [24]	3.09	4.72	29.70	3.28	3.29	4.30	8.31	5.61	6.00	21.80	2.84	3.09	9.00	2.36	10.90	7.22
BSM [25]	7.27	11.40	30.50	6.67	6.52	10.80	32.10	10.50	12.50	24.40	12.80	7.42	16.40	4.88	32.80	13.40
TestAD	11.72	15.21	38.45	9.38	8.50	15.40	37.15	14.25	15.55	29.30	15.72	9.21	20.70	7.54	36.68	19.25

TABLE II
THE COMPARISON RESULTS OF *all* ERROR USING THE MIDDLEBURY DATASET.

Algorithms	Adiron	ArtL	Jadepl	Motor	MotorE	Piano	PianoL	Pipes	Playrm	Playt	PlayP	Recyc	Shelvs	Teddy	Vintge	Weight Ave
Proposed Algorithm	4.79	7.68	27.30	6.26	6.12	6.67	13.20	11.30	7.73	20.10	6.10	3.90	8.99	3.60	9.64	9.09
SNCC [16]	3.63	6.78	39.80	5.12	5.11	4.65	8.23	11.80	8.05	45.60	4.36	3.29	8.10	2.55	14.80	10.40
ELAS [24]	4.08	7.18	52.80	5.39	5.45	4.96	9.00	10.70	7.94	23.20	3.83	3.78	9.46	3.34	11.60	10.60
MC-CNN [23]	4.24	18.70	34.10	7.21	7.22	6.00	9.35	13.50	18.30	9.71	9.37	4.64	6.62	9.35	21.60	11.80
BSM [25]	12.70	28.70	58.70	14.80	14.70	16.00	35.80	24.50	29.40	31.00	20.20	12.10	19.20	14.30	39.30	23.50
TestAD	17.32	29.88	63.45	16.90	16.54	18.40	37.19	27.65	32.55	35.00	22.84	15.32	22.25	17.60	43.25	28.20

[7] R. A. Hamzah, H. Ibrahim, and A. H. Abu Hassan, "Stereo matching algorithm based on illumination control to improve the accuracy," *Image Analysis & Stereology*, vol. 35, no. 1, pp. 39–52, 2016.

[8] M. G. Mozerov and J. van de Weijer, "Accurate stereo matching by two-step energy minimization," *IEEE Transactions on Image Processing*, vol. 24, no. 3, pp. 1153–1163, 2015.

[9] H. qian Wang, M. Wu, Y. bing Zhang, and L. Zhang, "Effective stereo matching using reliable points based graph cut," *Proceedings of Visual Communications and Image Processing*, pp. 1–6, 2013.

[10] X. Xiang, M. Zhang, G. Li, Y. He, and Z. Pan, "Real-time stereo matching based on fast belief propagation," *Machine Vision and Applications*, vol. 23, no. 6, pp. 1219–1227, 2012.

[11] K. He, J. Sun, and X. Tang, "Guided image filtering," *IEEE Transactions on Pattern Analysis and Machine Intelligence*, vol. 35, no. 6, pp. 1397–1409, 2013.

[12] R. A. Hamzah and H. Ibrahim, "Literature survey on stereo vision disparity map algorithms," *Journal of Sensors*, 2016.

[13] B. J. Tippetts, D.-J. Lee, J. K. Archibald, and K. D. Lillywhite, "Dense disparity real-time stereo vision algorithm for resource-limited systems," *IEEE Transactions on Circuits and Systems for Video Technology*,

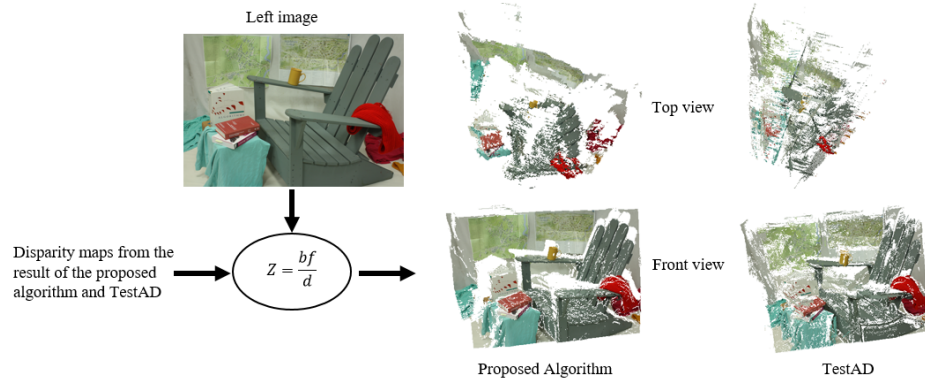


Fig. 4. The results of 3D surface reconstruction for one of the Middlebury image (i.e., Adirondack). The results are displayed with the front and top views.

- vol. 21, no. 10, pp. 1547–1555, 2011.
- [14] S. Satoh, “Simple low-dimensional features approximating ncc-based image matching,” *Pattern Recognition Letter*, vol. 32, no. 14, pp. 1902–1911, 2011.
- [15] W. Hu, K. Zhang, L. Sun, J. Li, Y. Li, and S. Yang, “Virtual support window for adaptive-weight stereo matching,” *International Conference on Computer Vision Theory and Applications*, pp. 1–4, 2011.
- [16] N. Einecke and J. Eggert, “Anisotropic median filtering for stereo disparity map refinement,” *International Conference on Computer Vision Theory and Applications*, pp. 189–198, 2013.
- [17] K.-J. Yoon and I. S. Kweon, “Adaptive support-weight approach for correspondence search,” *IEEE Transactions on Pattern Analysis and Machine Intelligence*, vol. 28, no. 4, pp. 650–656, 2006.
- [18] M. Michael, J. Salmen, J. Stallkamp, and M. Schlipsing, “Real-time stereo vision: Optimizing semi-global matching,” *IEEE Intelligent Vehicles Symposium*, pp. 1197–1202, 2013.
- [19] Z. Ma, K. He, Y. Wei, J. Sun, and E. Wu, “Constant time weighted median filtering for stereo matching and beyond,” *IEEE International Conference on Computer Vision*, pp. 49–56, 2013.
- [20] S. Ploumpis, A. Amanatiadis, and A. Gasteratos, “A stereo matching approach based on particle filters and scattered control landmarks,” *Image and Vision Computing*, vol. 38, pp. 13–23, 2015.
- [21] Z. Lee, J.-C. Juang, and T. Q. Nguyen, “Local disparity estimation with three-moded cross census and advanced support weight,” *IEEE Transactions on Multimedia*, vol. 15, no. 8, pp. 1855–1864, 2013.
- [22] D. Scharstein and R. Szeliski, “Middlebury stereo evaluation - version 3,” <http://vision.middlebury.edu/stereo/eval>. Accessed Date= 24 May 2016.
- [23] J. Zbontar and Y. LeCun, “Computing the stereo matching cost with a convolutional neural network,” in *IEEE Conference on Computer Vision and Pattern Recognition*, 2015, pp. 1592–1599.
- [24] A. Geiger, M. Roser, and R. Urtasun, “Efficient large-scale stereo matching,” in *Computer Vision (ACCV)*, 2011, pp. 25–38.
- [25] K. Zhang, J. Li, Y. Li, W. Hu, L. Sun, and S. Yang, “Binary stereo matching,” in *International Conference on Pattern Recognition (ICPR)*, 2012, pp. 356–359.